fortune Journals

Research Article

ARCHIVES OF
CLINICAL AND
BIOMEDICAL RESEARCH

ISSN: 2572-5017

Novel Ultrasound Liver Attenuation Imaging for Detection of Liver Steatosis: Comparison with MRI Based Imaging Methods with Liver Biopsy as A Reference Standard

Chileka Chiyanika[1,2], Kin Hung Liu[2], Vincent Wai-Sun Wong[3,4,5], Winnie Chiu Wing Chu[2*]

Abstract

Background and aim: Non-alcoholic fatty liver disease is a predominant cause of chronic liver disease worldwide. The aim of this study was to evaluate the performance of the novel ultrasound attenuation imaging (ATI) with MRI-proton density fat fraction (PDFF) and proton magnetic resonance spectroscopy (proton-MRS) in detecting and grading of liver steatosis, using liver biopsy as a reference standard.

Materials and methods: From March 2019 to September 2021, 15 adult subjects (age: 38 years, Male/female:5/10 females, BMI: 38.5kg/m^2) with morbid obesity planned for laparoscopic-sleeve-gastrectomy were recruited, and an intraoperative liver biopsy was performed. A control group of 8 healthy lean subjects (age: 25 years, Male/female: 4/4 females, BMI: 20.2kg/m^2) was also enrolled. ATI, MRI-PDFF, and proton-MRS were performed on the same day and within two weeks before surgery.

Results: Liver steatosis was present in 100% of the patients. ATI correlated with steatosis grade (r=0.833, p< 0.001). MRI-PDFF correlated with steatosis grade (r=0.926, p< 0.001) and non-alcoholic steatohepatitis activity score (r=0.820, p=0.001). ATI correlated with MRI-PDFF (r=0.885, p<0.001). AUROCs of ATI were 0.91, 0.97, and 0.93 for detecting steatosis grades 1,2, and 3 respectively.

Conclusions: ATI showed no significant d ifference in th e diagnostic performance when compared to MRI-PDFF and proton-MRS.

Keywords: Attenuation imaging; Liver steatosis; Liver biopsy; Magnetic resonance spectroscopy; Non-Alcoholic fatty liver disease; Proton density fat fraction.

Introduction

Non-alcoholic fatty liver disease (NAFLD) is a predominant cause of chronic liver disease worldwide and can progress from simple steatosis to non-alcoholic steatohepatitis (NASH), cirrhosis, and hepatocellular carcinoma (HCC) [1]. 12-40% of NAFLD patients develop NASH in 3-7 years [2, 3], while about 9-25% of patients with NASH develop cirrhosis over a period of 10-20 years [3]. In Asia, NAFLD is estimated at 30% of the adult population [4], globally; the prevalence is estimated at 24% and is increasing [5]. This increase is attributed to the association with obesity and insulin resistance [6,7].

Accurate detection and quantification of hepatic steatosis is therefore

Affiliation:
[1]Health Technology and Informatics, The Hong Kong Polytechnic University, Hong Kong, China.

[2]Department of Imaging and Interventional Radiology, Prince of Wales Hospital, The Chinese University of Hong Kong, Hong Kong, China.

[3]Institute of Digestive Disease, The Chinese University of Hong Kong, Hong Kong, China

[4]Medical Data Analytic Centre, The Chinese University of Hong Kong, Hong Kong, China

[5]Department of Medicine and Therapeutics, The Chinese University of Hong Kong, Hong Kong, China

***Corresponding author:**
Winnie Chiu Wing Chu. Department of Imaging and Interventional Radiology, Prince of Wales Hospital, The Chinese University of Hong Kong, Hong Kong, China.

Citation: Chileka Chiyanika, Kin Hung Liu, Vincent Wai-Sun Wong, Winnie Chiu Wing Chu. Novel Ultrasound Liver Attenuation Imaging for Detection of Liver Steatosis: Comparison with Mri Based Imaging Methods with Liver Biopsy As A Reference Standard. Archives of Clinical and Biomedical Research. 7 (2023): 527-536.

Received: August 29, 2023
Accepted: September 06, 2023
Published: October 03, 2023

Chiyanika C, et al., Arch Clin Biomed Res 2023
DOI:10.26502/acbr.50170368

clinically important. Liver biopsy is the gold standard for the diagnosis and grading of hepatic steatosis, but it is limited due to its invasiveness, sampling error, intra/inter observer variability, rare but life-threatening complications, and cost [8-10]. Conventional B-mode ultrasound is a widely used non-invasive imaging method, but it is subjective in estimating fatty liver infiltration based on sonographic features described by Scatarige et al [11]. Controlled attenuation parameter ultrasound technique has been developed with promising results [12] but limited due to high false positives and negatives rates, poorly standardised cut off values in hepatic steatosis, blind liver fat estimation (limiting the accuracy), estimation of liver fat is affected by skin to liver capsule ratio and requires a dedicated probe [12-14].

Chemical shift-based MRI methods such as proton density fat fraction (PDFF) and proton spectroscopy (proton-MRS) have been shown to be sensitive, accurate and reproducible methods to quantify hepatic steatosis [15]. However, MRI is expensive, has limited availability, and contraindicated in certain groups of patients. Novel ultrasound attenuation imaging (ATI) is based on the attenuation coefficient (AC) of the ultrasound beam in a tissue following the sum effects of scattering, diffusion, reflection, and absorption [16]. This AC corresponds to the change of the ultrasound beam intensity with depth. Thus, ATI has the potential to quantify fat in the liver, but very limited studies are available. Therefore, the aim of this study was to validate the novel ultrasound ATI in the detection and grading of NAFLD, using liver biopsy as a reference standard in morbid obese subjects, as well as to compare its diagnostic performance against MRI based imaging methods.

Materials and methods:

Study Participants

This cross-sectional study was part of the prospective study investigating the biological impact on morbid obese Chinese subjects before and after bariatric surgery. Between March 2019 to February 2022, fifteen (15) obese subjects planned for laparoscopic sleeve gastrectomy were invited and recruited to participate in this study after fulfilling the selection criteria. Further, eight (8) lean healthy control subjects were recruited into the study. The protocol of this study was reviewed and approved by the Clinical Research Ethics Committee (reference number 2018.612). Written informed consent was obtained from all the participants.

Selection Criteria

Inclusion criteria was as follows for the treatment group: age 18-65 years, and of Chinese ethnicity, BMI ≥ 32.5 kg/m^2 (adjusted criteria for Asian population [17,18]), presence of NAFLD based on MRI PDFF ≥ 5.5%, availability of liver biopsy results following an intra-operative liver biopsy during bariatric surgery as part of the protocol. The inclusion criteria for the control group was: age 18-30 years, and of Chinese ethnicity, BMI ≤ 23kg/m^2, absence of NAFLD based on MRI PDFF < 5.5%. It is acknowledged here that the inclusion criteria for the control group was not age-matched with the intervention group because we aimed at getting the true liver attenuation coefficient values in subjects with absolutely low liver fat content, especially that liver fat content accumulation is exponential with age. Exclusion Criteria included: any contraindications to MRI, other kind of hepatic diseases or under medications known to affect liver fat accumulation, and excessive alcohol consumption (>30g/d for men and >20g/d for women).

Clinical And Anthropometric Measurements

Anthropometric measurements including body weight, height, waist and hip circumferences, diastolic and systolic blood pressures were recorded. BMI was calculated as weight in kilograms (kg) divided by height in meter squared (m^2). BMI was then used to categorise obesity status of the subjects using the World Health Organization region specific classification of weight [17,18]. Blood tests including liver enzymes, glucose, and lipids were conducted after 8 hours of fasting. The clinical, anthropometrics, and blood tests were done on the day of operation (surgery).

Insulin Resistance/ Type 2 Diabetes Mellitus (T2DM)

Insulin resistance was estimated by homeostasis model assessment- insulin resistance (HOMA-IR), using the formulae: HOMA-IR = fasting plasma glucose (mmol/L) x insulin (mIU/L) / 22.5 [19]. Insulin resistance was defined as HOMA-IR ≥ 1.4 in non-diabetic subjects and ≥ 2.0 in diabetic subjects [20]. The diagnosis of T2DM was based on the criteria set by World health Organization [21].

Metabolic Syndrome

Metabolic syndrome was based on the Harmonized criteria [22] i.e., the presence of at least any three of five of the following: (1) central obesity (waist circumference ≥90cm in Asian men and ≥80cm in Asian women); (2) triglycerides ≥1.7mmol/l; (3) reduced high-density lipoprotein-cholesterol (<1.0 mmol/l in men and <1.3 mmol/l in women); (4) blood pressure ≥130/85mmHg; and (5) fasting plasma glucose ≥5.6mmol/l, or receiving treatment for any of the above metabolic abnormalities.

Bariatric Surgery

Two experienced bariatric surgeons performed the laparoscopic sleeve gastrectomy procedure in accordance with the departmental standard protocols. All the surgical subjects received routine follow-up in accordance with the departmental standard treatment guidelines.

Chiyanika C, et al., Arch Clin Biomed Res 2023
DOI:10.26502/acbr.50170368

Liver Biopsy

Intraoperative liver biopsy (mostly from the left lobe) was performed by two experienced bariatric surgeons (blinded to MRI data) during the bariatric surgery procedure in all the subjects using a Temno bevel tip needle, 16Gx15cm. The biopsied liver tissue specimen of each subject was fixed in formalin solution. Using the departmental standard

protocols, the Pathologist examined the specimen and the NASH Clinical Research Network (CRN) NAFLD activity score and fibrosis staging was used as follows [23]: Non-alcoholic steatohepatitis activity score (NAS:0-8) i.e., hepatic steatosis (grade 0-3), lobular inflammation (grade 0-3), and ballooning (grade 0-2). Liver fibrosis staging (stage 0-4) was also performed using the Brunt's fibrosis grading scale.

Imaging Studies

Imaging studies including ultrasound and MRI were performed in all 15 subjects on the same day, and within two weeks from surgery. All subjects fasted for at least 6 hours before the exams. Additionally, 8 healthy lean control subjects were also subjected to ultrasound liver ATI and MRI examinations.

Ultrasound Liver Attenuation Imaging

An Aplio i800, Canon medical systems, Tochigi, Japan ultrasound machine was used. Using a 1 to 8MHz convex transducer (i8CX1), the liver parenchyma was first evaluated on B-mode to ensure that the fan shaped sampling box was placed in a homogenous region, thereafter the ATI mode was activated. All images were obtained in the supine position and in the intercostal planes with the transducer perpendicular to the skin. An approximately 4 x 8cm sampling box was positioned randomly in the liver (including the left lobe), 2 cm below the capsule during several seconds of breath-holding. Non-homogeneous areas such as large vessels and cystic structures were automatically excluded from the ATI map using a system inherent structure removal filter. Thus, homogenous ATI colour maps were acquired as much as possible.

By careful avoidance of large vessels and areas of reverberation artifacts, a 2 x 4cm region of interest for measurement was set within the sampling box of ATI and placed in the middle portion of the sampling box to reduce the intra-observer variability as shown in Figure1. Attenuation coefficient with $R^2 \geq 0.92$ was regarded as valid measurement. ATI examinations were performed until five valid AC (dB/cm/MHz) measurements were obtained and the median value of the measurements was used for analysis. The intraclass correlation coefficient was calculated to assess the reliability of the measurements.

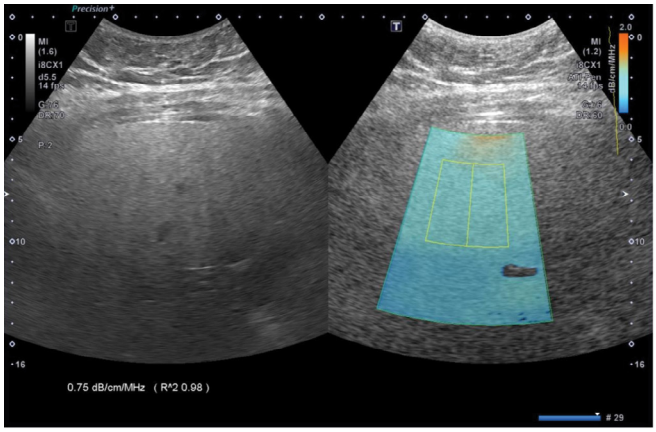

Figure 1: Two-dimensional ultrasound attenuation imaging in a 38-year-old woman. Simultaneous display of B-mode ultrasound image (left) and a color-coded attenuation map (right). A system inherent structure removal filter removes areas of significant errors in attenuation calculation (e.g., large vessels). Coefficient of determination (R^2 value) and attenuation are displayed in each acquisition.

MRI Data Acquisition and Analysis

A Philips Achieva 3.0T MRI Scanner (Philips Medical System, Best, The Netherlands) equipped with a 16-channel SENSE-XL-Torso array coil was used.

Chemical Shift Encoded Proton Density Fat Fraction (PDFF)

Chemical-shift water-fat images were acquired by the 3D spoiled multi-echo mDIXON sequence to yield co-registered water, fat, fat-fraction and T2* image series. Imaging parameters were as follows: TR = 5.7-5.9 (ms), TE/echo spacing = 1.2-1.4 (ms) / 1.0-1.2 (ms), number of echoes = 6, flip angle = 3°, SENSE acceleration = 2, reconstructed slice thickness/number of slices = 4.0 mm / 50. A 15 second breath-hold acquisition of the liver was acquired. Data were exported for offline analysis using a Philips DICOM Viewer version R3.0-SP15, Philips Healthcare, Netherlands to determine the liver PDFF for each subject. Nine elliptical regions of interest (ROIs) of $4cm^2$ were placed on each of the nine Couinaud liver segments based on PDFF maps, while avoiding hepatic blood vessels, bile ducts, and motion artifacts. The mean PDFF from all the nine ROIs was used for analysis, and PDFF ≥ 5.5% was used to define fatty liver.

Liver Fat Content Measurements with Proton Magnetic Resonance Spectroscopy (Proton-MRS)

A STEAM spectroscopy sequence (TR = 5,000 ms, TE = 15 ms, NSA = 24, data points = 2,048, spectral width = 2,000 Hz) of the liver was performed in the same scan using the torso coil to acquire a spectrum of intrahepatic triglycerides (IHTG). A 30 x 30 x 30 mm^3 voxel was placed

Chiyanika C, et al., Arch Clin Biomed Res 2023
DOI:10.26502/acbr.50170368

Table 1: Characteristics of the subjects based on steatosis grade by histology.

Characteristics	All subjects (n=15)	Steatosis grade 1 (n=4)	Steatosis grade 2 (n=7)	Steatosis grade 3 (n=4)	P-value
Age (year)	38 (28-50)	43 (38-50)	37 (28-48)	38 (37-43)	0.185
BMI (Kg/m^2)	38.5 (30.9-44.6)	38.7 (33.6-40.6)	38.3 (30.9-44.6)	40.0 (36.1-43.3)	0.736
Waist circumference (cm)	115 (95-127)	120 (110-125)	115 (95-127)	115 (114-116)	0.542
WC/HIP ratio	0.94 (0.85-1.06)	0.94 (0.89-0.98)	0.95 (0.85-1.02)	0.96 (0.87-1.06)	0.865
Systolic blood pressure (mm Hg)	128 (102-1400	130 (102-132)	129 (107-140)	127 (125-129)	0.957
Diastolic blood pressure (mm Hg)	68 (57-87)	66 (57-86)	68 (59-86)	82 (76-87)	0.327
Antihypertensive drugs, n (%)	8 (57.1)	2 (50)	3 (42.9)	3 (75)	0.820
Total cholesterol (mmol/L)	4.40 (0.60-6.10)	4.95 (3.20-6.10)	4.20 (0.60-5.00)	4.90 (4.00-5.40)	0.320
Triglycerides (mmol/L)	1.50 (0.80-2.40)	1.55 (1.00-1.60)	1.40 (1.20-2.40)	1.05 (0.80-2.40)	0.394
HDL-c (mmol/L)	1.20 (0.90-2.20)	1.30 (0.90-1.30)	1.20 (0.90-2.20)	1.30 (1.00-1.50)	0.866
LDL-c (mmol/L)	2.60 (1.20-4.50)	3.10 (1.20-4.50)	2.50 (2.00-2.80)	2.85 (2.20-3.80)	0.176
Albumin (mmol/L)	40 (36-43)	39 (36-42)	40 (36-43)	40 (39-42)	0.945
Lipid lowering drugs, n (%)	4 (28.6)	1 (25)	2 (28.6)	1 (25)	1.000
HBA1c (%)	6.30 (5.50-11.60)	5.85 (5.40-5.90)	6.40 (5.60-11.60)	6.55 (5.90-7.10)	0.421
Fasting plasma glucose (mmol/L)	5.90 (4.60-9.20)	5.80 (5.40-5.90)	5.80 (4.60-9.20)	6.30 (5.30-8.60)	0.645
Plasma fasting Insulin (mIU/L)	22.65 (12.80-42.90)	25.50 (20.50-28.60)	21.00 (12.80-42.92)	15.30 (15.30-15.30)	0.693
HOMA-IR	6.03 (4.35-20.53)	6.56 (4.92-7.50)	5.75 (4.35-9.72)	12.51 (4.49-20.53)	0.847
Insulin resistance, n (%)	15 (100	4 (100)	7 (100)	4 (100)	1.000
Diabetes, n (%)	9 (60)	2 (50)	4 (57.1)	3 (75)	1.000
Antidiabetic drug, n (%)	9 (64.3)	2 (50)	4 (57.1)	3 (75)	1.000
Metabolic syndrome, n (%)	11 (73.3)	2 (50)	5 (71.5)	4 (100)	0.303
ALP (IU/L)	76 (49-103)	67 (55-84)	91 (50-103)	61 (49-69)	0.109
ALT (IU/L)	39 (18-69)	34 (18-37)	39 (20-64)	68 (46-69)	0.107
AST (IU/L)	28 (16-78)	25 (20-45)	26 (16-40)	47 (29-78)	0.053
AST/ALT ratio	0.69 (0.42-1.11)	0.69 (0.42-1.11)	0.67 (0.42-0.95)	0.74 (0.43-0.98)	0.803
GGT (IU/L)	48 (30-65)	37 (30-65)	49 (31-65)	50 (43-61)	0.509
MRS (%)	21.37 (7.11-53.77)	21.03 (7.11-22.58)	28.44 (15.94-53.77)	45.73 (42.13-49.33)	0.158
PDFF (%)	14.66 (4.82-32.48)	10.95 (4.82-15.82)	19.90 (11.34-26.70)	30.60 (28.71-32.48)	0.027
ATI (dB/cm/mHz)	0.68 (0.55-1.03)	0.59 (0.55-0.63)	0.68 (0.63-0.76)	0.71 (0.66-1.03)	0.075

Kruskal-Wallis test. BMI=body mass index, WC=waist circumference, HDL-c= high density lipoprotein cholesterol, LDL-c=low density lipoprotein cholesterol, HOMA-IR= homeostasis model assessment-insulin resistance, HBA1c= glycated haemoglobin, ALP=alkaline phosphatase, ALT=alanine aminotransferase, AST=aspartate aminotransferase, GGT= gamma glutamyl transferase, NASH= non-alcoholic steatohepatitis, MRS= Magnetic resonance spectroscopy, MRI PDFF= Magnetic resonance imaging proton density fat fraction, ATI= attenuation imaging, CCA IMT= common carotid artery intima-media thickness.

Citation: Chileka Chiyanika, Kin Hung Liu, Vincent Wai-Sun Wong, Winnie Chiu Wing Chu. Novel Ultrasound Liver Attenuation Imaging for Detection of Liver Steatosis: Comparison with Mri Based Imaging Methods with Liver Biopsy As A Reference Standard. Archives of Clinical and Biomedical Research. 7 (2023): 527-536.

Chiyanika C, et al., Arch Clin Biomed Res 2023
DOI:10.26502/acbr.50170368

in the right liver lobe (Couinaud segment V–VIII). A survey was performed to help in positioning the voxel and avoiding major vessels. Short TE and long TR were selected to minimize T2 and T1 effects. A non-breath-hold scan was performed, with the acquisition time of approximately 2 minutes. Data were exported for offline spectral analysis using the jMRUI software package [24]. Single lipid peaks seen at 0.90ppm, 1.30ppm and 2.1ppm were measured for relative fat signal integrals in terms of a percentage of the total signal amplitude. IHTG content was calculated using

$$FF\ (\%)\frac{Signal\ intensity\ of\ fat}{Sum\ of\ signal\ intensity\ of\ fat\ and\ water}\ x\ 100.$$

Statistical Analysis

Data were expressed as median (interquartile range), unless stated otherwise. Both Pearson's and Spearman's correlation coefficients were used accordingly to test the relationship between hepatic fat content as obtained from biopsy, ATI, MRI-PDFF, and proton-MRS. Correlation coefficients were categorized as: negligible (0.00-0.10), weak (0.10-0.39), moderate (0.40-0.69), strong (0.70-0.89) and very strong (0.90-1.00) [20]. The intraclass correlation coefficient was utilised to assess the reliability and repeatability of measurements. Kruskal-Wallis and Mann-Whitney tests were used to compare groups accordingly. Area under receiver operating characteristic (AUROC) curve was used to test the diagnostic performance of the imaging methods. Pairwise comparisons of AUROC of the imaging methods were performed using the DeLong test. All tests were two-sided and p-values <0.05 were considered significant.

Results

Patient Characteristics

Fifteen subjects (5 males and 10 females; median age, 38 years, age range 28-50 years; median BMI, 38.5kg/m^2, BMI range 30.9-44.6kg/m^2) were analysed. All subjects (100%) had liver steatosis confirmed by histology. Subject distribution per steatosis grade was as follows: 4 (26.7%) subjects had grade 1 steatosis, 7 (46.7%) subjects had steatosis grade 2, and 4 (26.7%) subjects had steatosis grade 3 (Table1). NASH was present in 6 (40%) subjects, spotty necrosis was present in 14 (93.3%) subjects, hepatocyte ballooning was present in 6 (40%) subjects and fibrosis was present in 9 (60%) subjects (Table 1).

Associations between histology score and imaging methods

ATI showed a strong association with histology steatosis grade (r= 0.833, p<0.001), but not with non-alcoholic steatohepatitis (NAS) activity score (r= 0.600, p=0.067) and fibrosis stage (r=0.285, p=0.424). Similarly, MRI-PDFF showed a very strong association with histology steatosis grade (r=0.926, p< 0.001) and a strong association with NAS activity score (r=0.820, p=0.001) but not with fibrosis stage (r=0.016, p=0.962). Proton-MRS showed a strong association with histology steatosis grade (r=0.874, p<0.001) but not with NAS activity score and fibrosis stage (r=0.405, p= 0.192; and r= -0.268, p= 0.399, respectively). The intra class correlation coefficient (ICC) achieved in the measurements of ATI was: 0.936 (95% [CI]: 0.805-0.980, p< 0.001).

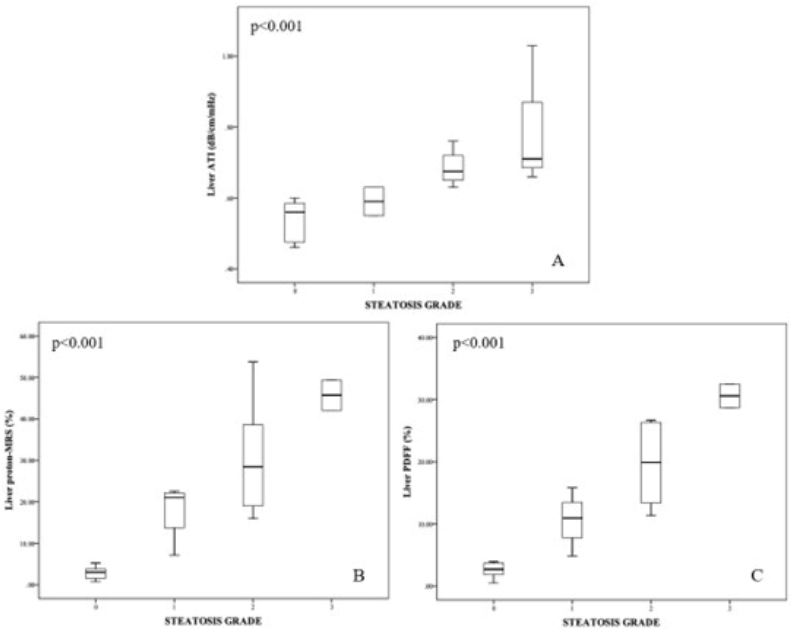

Figure 2: Linear by linear association of various imaging methods according to liver steatosis grade on histology (A= ATI, B= MRI-PDFF, C=proton-MRS).

Citation: Chileka Chiyanika, Kin Hung Liu, Vincent Wai-Sun Wong, Winnie Chiu Wing Chu. Novel Ultrasound Liver Attenuation Imaging for Detection of Liver Steatosis: Comparison with Mri Based Imaging Methods with Liver Biopsy As A Reference Standard. Archives of Clinical and Biomedical Research. 7 (2023): 527-536.

Chiyanika C, et al., Arch Clin Biomed Res 2023
DOI:10.26502/acbr.50170368

Linear by linear association showed that ATI, MRI-PDFF and proton-MRS (All, p<0.001) significantly increased with the increase in steatosis grade as shown in Figure 2. Interestingly, it was shown that the median AC (range) between those with steatosis grade 0 {0.56 (0.46-0.60dB/cm/MHz)} and steatosis grade 1 {0.59 (0.55-0.63 dB/cm/MHz)} were not significantly different (p=0.432), with an overlap in the AC range between them. However, this outcome was not observed in MRI-PDFF, and proton-MRS methods as shown in Table 2.

Associations Among Imaging Methods

ATI showed a strong positive association with MRI-PDFF (r=0.885, p<0.001) as well as proton-MRS (r=0.836, p<0.001), whereas there was a very strong positive association between MRI-PDFF and proton-MRS (r=0.970, p<0.001).

Diagnostic Performance

The AUROCs of ATI were 0.91 (0.67-1.00, p<0.001, for grade 0 (i.e., S0 vs. S1-3), 0.97 (0.74-1.00, p<0.001, for

Table 2: Anthropometric and imaging characteristics of subjects in the control and intervention groups

Characteristics	Control group	Intervention group (n=15)			
	Steatosis grade 0 (n=8)	All (n=15)	Steatosis grade 1 (n=4)	Steatosis grade 2 (n=7)	Steatosis grade 3(n=4)
Age (year)	25 (22-30)	38 (28-50)	43 (38-50)	37 (28-48)	38 (37-43)
BMI (Kg/m^2)	20.2 (17.4-23.1)	38.5 (30.9-44.6)	38.7 (33.6-40.6)	38.3 (30.9-44.6)	40.0 (36.1-43.3)
Liver proton-MRS (%)	3.04 (0.71-5.22)	21.37 (7.11-53.77)	21.03 (7.11-22.58)	28.44 (15.94-53.77)	45.73 (42.13-49.33)
Liver MRI-PDFF (%)	2.71 (0.47-3.97)	15.32 (10.76-32.48)	11.14 (10.76-15.82)	19.90 (11.34-26.70)	30.60 (28.71-32.48)
Liver ATI (dB/cm/MHz)	0.56 (0.46-0.60)	0.68 (0.55-1.03)	0.59 (0.55-0.63)	0.68 (0.63-0.76)	0.71 (0.66-1.03)

Mann-Whitney U test. BMI=body mass index, WC=waist circumference, NASH= non-alcoholic steatohepatitis, MRS= Magnetic resonance spectroscopy, MRI PDFF= Magnetic resonance imaging proton density fat fraction, ATI= attenuation imaging.

Table 3: Diagnostic accuracy test results of the imaging methods for different liver steatosis grades

STEATOSIS GRADE	IMAGING METHOD	Cut-off	AUROC	Youden index J	Sensitivity (%)	Specificity (%)	P-value
S0 vs. S1-S3	ATI	>0.59 dB/cm/MHz	0.91 (0.67-1.00)	0.75	87.5 (47.3-99.7)	87.5 (47.3-99.7)	<0.001
(S>0)	MRI-PDFF	>3.97%	1.00 (0.82-1.00)	1	100 (71.5-100)	100 (63.1-100)	<0.001
	Proton MRS	>5.22%	1.00 (0.82-1.00)	1	100 (71.5-100)	100 (63.1-100)	<0.001
S0-S1 vs. S2-S3	ATI	>0.60 dB/cm/MHz	0.97 (0.74-1.00)	0.8	83.3 (35.9-99.6)	90.0 (55.5-99.7)	<0.001
(S>1)	MRI-PDFF	>11.14%	0.97 (0.77-1.00)	0.91	100 (63.1-100)	90.9 (58.7-99.8)	<0.001
	Proton MRS	>5.22%	0.91 (0.69-0.99)	0.73	100 (63.1-100)	72.7 (39.0-94.0)	<0.001
	ATI	>0.63 dB/cm/MHz	0.93 (0.69-1.00)	0.86	100 (15.8-100)	85.7 (57.2-98.2)	<0.001
S0-S2 vs. S3	MRI-PDFF	>26.3%	0.97 (0.77-1.00)	0.94	100 (15.8-100)	94.1 (71.3-99.9)	<0.001
(S>2)	Proton MRS	>38.6%	0.94 (0.73-1.00)	0.94	100 (15.8-100)	94.1 (71.3-99.9)	<0.001

Parenthesis (brackets) =95% confidence interval. ATI= attenuation coefficient, MRI-PDFF= Magnetic resonance imaging- proton density fat fraction. Proton MRS= proton magnetic resonance spectroscopy, AUROC= area under receiver operating characteristic curve, dB= decibel. S=steatosis grade.

Citation: Chileka Chiyanika, Kin Hung Liu, Vincent Wai-Sun Wong, Winnie Chiu Wing Chu. Novel Ultrasound Liver Attenuation Imaging for Detection of Liver Steatosis: Comparison with Mri Based Imaging Methods with Liver Biopsy As A Reference Standard. Archives of Clinical and Biomedical Research. 7 (2023): 527-536.

Chiyanika C, et al., Arch Clin Biomed Res 2023
DOI:10.26502/acbr.50170368

Table 4: Pairwise comparisons of area under receiver operating characteristic curves of the imaging methods for detecting various hepatic steatosis grades.

ATI vs. PDFF	**S0 vs. S1-S3 (S>0)**	**S0-S1 vs. S2-S3 (S>1)**
Difference between areas	0.0982	0.04
Standard Error [a]	0.0932	0.0422
95% Confidence Interval	-0.0845 to 0.281	-0.0428 to 0.123
z statistic	1.054	0.947
Significance level	p=0.292	p = 0.344
ATI vs. MRS		
Difference between areas	0.0982	0.08
Standard Error [a]	0.0932	0.0951
95% Confidence Interval	-0.0845 to 0.281	-0.106 to 0.266
z statistic	1.054	0.841
Significance level	p=0.292	p = 0.400
PDFF vs. MRS		
Difference between areas	0	0.12
Standard Error [a]	0	0.0938
95% Confidence Interval	-	-0.0639 to 0.304
z statistic	-	1.279
Significance level	p=1.000	p = 0.201

[a]DeLong test. ATI= attenuation imaging, MRS= magnetic resonance spectroscopy, PDFF= proton density fat fraction, S=steatosis grade.

grade 1 (S0-1 vs. S2-3), and 0.93 (0.69-1.00, p<0.001, for grade 2 (S0-2 vs. S3). The corresponding Youden's index, sensitivity, specificity as well as the AUROCs of MRI-PDFF and proton-MRS are shown in Table 3.

There were no significant differences on pairwise comparison of the AUROCs of the imaging methods (ATI, MRI-PDFF and proton-MRS) for detecting S> grade 0 and S> grade 1, as summarised in Table 4. Due to limited sample size, data were insufficient for a pairwise comparison of the AUROCs for detecting S> grade 2.

Discussion

In this study, ATI showed a significant correlation with MRI-PDFF, and proton-MRS. ATI also showed a significant correlation with liver steatosis grade as determined by histology, but not with NAS activity score and fibrosis stage. The diagnostic performance of ATI for detecting liver steatosis greater than grades 0,1 and 2 were 0.91, 0.97 and 0.93, respectively. The diagnostic performance of ATI, MRI-PDFF and proton-MRS were shown not to be significantly different in detecting various liver steatosis grades. The strength of this study lies in the use of subjects who had liver biopsy and within a short interval between biopsy and imaging. The success of ATI in this morbid obese cohort with liver steatosis without any other underlying liver pathologies is another strength. The comparison of ATI with both MRI-PDFF and proton-MRS which has not been assessed in previous studies further adds to the strength of the study.

ATI showed a strong correlation with steatosis grade (r=0.833). Bae et al [25]. in a study involving 108 patients with histology proven steatosis showed the correlation coefficient of ATI with steatosis grade of 0.660. Likewise, Tamaki et al [26] in a study involving 351 patients showed a correlation coefficient of 0.470. Similarly, Huang et al [27] showed a correlation of 0.721 between ATI and steatosis grade. Variations in the correlation coefficients in these studies could be attributed to the varying BMIs, sample sizes, mixed liver aetiologies, and ethnicities used. Moreover, Nazare et al [28] showed that ethnicity significantly affects liver fat distribution, while Fan et al [29] showed that BMI (even in dose dependent manner) was associated with fatty liver risk. Indeed, our study cohort had no known other liver pathologies as was in other studies. It was further shown that ATI did not correlate with NAS activity score and fibrosis stage, in agreement with previous studies [25,26]. These outcomes may imply that ATI may not be affected by inflammation/fibrosis and therefore a poor marker for both conditions, yet it reassures that ATI seems to only determine the fat content in the liver without being affected by the presence of inflammation/fibrosis. However, more studies linking ATI with necroinflammatory activity score, or fibrosis stage are needed to confirm this outcome.

In this study, the diagnostic accuracy (AUROC) of ATI in detecting liver steatosis grades 1, 2 and 3 were 0.91, 0.97 and 0.93 respectively. The associated AC cut-off points for the above steatosis grades were: 0.59cm/dB/MHz, 0.60cm/dB/MHz, and 0.63cm/dB/MHz, respectively. These outcomes are similar to previous studies [16, 25, 26, 30-37]. It was also shown that pairwise comparison of AUROCs of the imaging methods did not show any significant differences. These results suggest that ATI may be a useful non-invasive tool to quantify liver steatosis. They further imply that ATI may be a reliable method to quantify hepatic fat even in subjects with morbid obesity, and its usefulness may enable early detection of liver steatosis at a relatively low cost. This could allow "mass screening" to be possible for purposes of either general population studies on NAFLD or for early detection of liver steatosis. This might particularly be helpful in encouraging lifestyle changes before marked hepatic damage occurs. However, the AC range of steatosis grade 0 was shown to overlap with the AC range of steatosis grade 1, unlike the outcome of both MRI-PDFF and proton-MRS. Like our findings, we also noticed this overlap in previous studies [16,25,26,30-37]. These outcomes suggest that ATI may not be as sensitive as MRI-PDFF/proton-MRS for distinguishing between steatosis grades 0 and 1, and care must be taken when using ATI as some cases may be allocated as being

Chiyanika C, et al., Arch Clin Biomed Res 2023
DOI:10.26502/acbr.50170368

positive or negative when in fact not. Under such suspicious circumstances, MRI-PDFF can be used to confirm the outcome. Notwithstanding the above argument, ATI seems to be reasonably more sensitive in detecting severe forms of steatosis (grades 2 and 3).

Our study, together with previous studies showed a variation in AC cut-off points for various steatosis grades (i.e., 0.56- 0.63cm/dB/MHz for steatosis > 0; 0.59-0.72cm/dB/MHz for steatosis > 1; and 0.69-0.94cm/dB/MHz for steatosis > 2) [16, 26, 30, 32, 34, 38-40]. This variation in AC cut-off points in these studies could in part be explained by use of transducers of varying frequencies (mostly 3 and 4MHz as reference frequencies), especially that attenuation is directly related to transducer frequency (the higher the frequency, the higher the attenuation). However, this variation further suggests that presently, ATI has no standardised cut-off points as is the case with MRI, hence the need for more validation studies involving large sample sizes, in multiple centres, and using a homogenous transducer reference frequency.

The major limitation of this study is the small sample size, which could account for our findings, and this was because of COVID-19 pandemic as all elective surgical cases were suspended. However, the results obtained in this study are comparable to few available studies on ATI which had larger sample sizes, thus, care must be exercised when interpreting these results. ATI examinations were conducted by a single operator, thus, interobserver agreement could not be assessed. Nonetheless, inter-observer correlation of ATI has been shown to range from 0.91-0.98 [13, 33, 41-44]. Finally, the cohort was of Chinese ethnicity, therefore, caution should be taken in the generalisation of the results.

Conclusion

ATI is a promising non-invasive tool in quantifying hepatic fat, whose diagnostic performance is not significantly different to MRI-PDFF and proton-MRS. Future multicentre studies with large sample sizes in subjects with histologically proven liver steatosis and a control group may be needed to further validate this modality, especially that currently there is non-availability of standardized attenuation coefficient cut-off values for each corresponding steatosis grade in various ethnic groups and BMIs.

Author Contributions

The roles of CC in the study were: conceptualization, data curation, formal analysis, investigation, methodology. WC roles were in: methodology, project administration, resources, supervision, writing, review & editing. KHL roles were in: investigation, supervision, writing, review & editing. VW roles were in: validation, writing, review & editing, supervision. CC and WC were involved in investigation and analysis. WC sourced the project funding. All authors agreed to be accountable for all aspects of the work.

Acknowledgements

The authors are grateful to the staff at the Chinese University of Hong Kong- Prince of Wales Hospital (CUHK-PWH) Multidisciplinary Clinic of Metabolic & Bariatric Surgery (MCMBS) and Radiology department for their contributions. The authors also thank all the participants in the study.

Conflicts of interest: None to report

References

1. Szczepaniak LS, Nurenberg P, Leonard D, et al. Magnetic resonance spectroscopy to measure hepatic triglyceride content: Prevalence of hepatic steatosis in the general population. American Journal of Physiology-Endocrinology and Metabolism 288 (2005): 462-468.
2. Estes C, Anstee QM, Arias-Loste MT, et al. Modeling nafld disease burden in china, france, germany, italy, japan, spain, united kingdom, and united states for the period 2016–2030. J Hepatol 69 (2018): 896-904.
3. Kumar R, Priyadarshi RN, Anand U. Non-alcoholic fatty liver disease: Growing burden, adverse outcomes and associations. Journal of Clinical and Translational Hepatology 8 (2020): 76.
4. Li J, Zou B, Yeo YH, et al. Prevalence, incidence, and outcome of non-alcoholic fatty liver disease in asia, 1999–2019: A systematic review and meta-analysis. The lancet Gastroenterology & hepatology 4 (2019): 389-398.
5. Younossi ZM, Koenig AB, Abdelatif D, et al. Global epidemiology of nonalcoholic fatty liver disease—meta-analytic assessment of prevalence, incidence, and outcomes. Hepatology 64 (2016): 73-84.
6. Chalasani N, Younossi Z, Lavine JE, et al. The diagnosis and management of nonalcoholic fatty liver disease: Practice guidance from the american association for the study of liver diseases. Hepatology 67 (2018): 328-357.
7. European Association for the Study of the Liver, European Association for the Study of Diabetes, (EASD. EASL-EASD-EASO clinical practice guidelines for the management of non-alcoholic fatty liver disease. Obesity facts 9 (2016): 65-90.
8. Angulo P. Nonalcoholic fatty liver disease. N Engl J Med 346 (2002): 1221-1231.
9. Bedossa P, Dargère D, Paradis V. Sampling variability of liver fibrosis in chronic hepatitis C. Hepatology 38 (2003): 1449-1457.

Chiyanika C, et al., Arch Clin Biomed Res 2023
DOI:10.26502/acbr.50170368

10. French METAVIR Cooperative Study Group, Bedossa P. Intraobserver and interobserver variations in liver biopsy interpretation in patients with chronic hepatitis C. Hepatology 20 (1994): 15-20.

11. Scatarige JC, Scott WW, Donovan PJ, et al. Fatty infiltration of the liver: Ultrasonographic and computed tomographic correlation. Journal of Ultrasound in Medicine 3 (1984): 9-14.

12. Pirmoazen AM, Khurana A, El Kaffas A, et al. Quantitative ultrasound approaches for diagnosis and monitoring hepatic steatosis in nonalcoholic fatty liver disease. Theranostics 10 (2020): 4277.

13. Tada T, Iijima H, Kobayashi N, et al. Usefulness of attenuation imaging with an ultrasound scanner for the evaluation of hepatic steatosis. Ultrasound Med Biol 45 (2019): 2679-2687.

14. Zhang YN, Fowler KJ, Hamilton G, et al. Liver fat imaging—a clinical overview of ultrasound, CT, and MR imaging. Br J Radiol 91 (2018):20170959.

15. Wong VW, Adams LA, de Lédinghen V, et al. Noninvasive biomarkers in NAFLD and NASH—current progress and future promise. Nature reviews Gastroenterology & hepatology 15 (2018): 461-478.

16. Tada T, Iijima H, Kobayashi N, et al. Usefulness of attenuation imaging with an ultrasound scanner for the evaluation of hepatic steatosis. Ultrasound Med Biol 45 (2019): 2679-2687.

17. Fan J, Kim S, Wong VW. New trends on obesity and NAFLD in asia. J Hepatol 67 (2017): 862-873.

18. Consultation WE. Appropriate body-mass index for asian populations and its implications for policy and intervention strategies. Lancet (London, England) 363 (2004): 157-163.

19. Matthews DR, Hosker JP, Rudenski AS, et al. Homeostasis model assessment: Insulin resistance and β-cell function from fasting plasma glucose and insulin concentrations in man. Diabetologia 28 (1985): 412-419.

20. Lee CH, Shih A, Woo YC, et al. Optimal cut-offs of homeostasis model assessment of insulin resistance (HOMA-IR) to identify dysglycemia and type 2 diabetes mellitus: A 15-year prospective study in chinese. PloS one 11 (2016): 0163424.

21. World Health Organization. Definition and diagnosis of diabetes mellitus and intermediate hyperglycaemia: Report of a WHO/IDF consultation (2006).

22. Alberti K, Eckel RH, Grundy SM, et al. Harmonizing the metabolic syndrome: A joint interim statement of the international diabetes federation task force on epidemiology and prevention; national heart, lung, and blood institute; american heart association; world heart federation; international atherosclerosis society; and international association for the study of obesity. Circulation 120 (2009): 1640-1645.

23. Kleiner DE, Brunt EM, Van Natta M, et al. Design and validation of a histological scoring system for nonalcoholic fatty liver disease. Hepatology 41 (2005): 1313-1321.

24. Stefan D, Di Cesare F, Andrasescu A, et al. Quantitation of magnetic resonance spectroscopy signals: The jMRUI software package. Measurement Science and Technology 20 (2009): 104035.

25. Bae JS, Lee DH, Lee JY, et al. Assessment of hepatic steatosis by using attenuation imaging: A quantitative, easy-to-perform ultrasound technique. Eur Radiol 29 (2019): 6499-6507.

26. Tamaki N, Koizumi Y, Hirooka M, et al. Novel quantitative assessment system of liver steatosis using a newly developed attenuation measurement method. Hepatology Research 48 (2018): 821-828.

27. Huang Y, Bian H, Zhu Y, et al. Quantitative diagnosis of nonalcoholic fatty liver disease with ultrasound attenuation imaging in a biopsy-proven cohort. Acad Radiol (2023).

28. Nazare J, Smith JD, Borel A, et al. Ethnic influences on the relations between abdominal subcutaneous and visceral adiposity, liver fat, and cardiometabolic risk profile: The international study of prediction of intra-abdominal adiposity and its relationship with cardiometabolic risk/ intra-abdominal adiposity. Am J Clin Nutr 96 (2012): 714-726.

29. Fan R, Wang J, Du J. Association between body mass index and fatty liver risk: A dose-response analysis. Scientific reports 8 (2018): 1-7.

30. Ferraioli G, Maiocchi L, Raciti MV, et al. Detection of liver steatosis with a novel ultrasound-based technique: A pilot study using MRI-derived proton density fat fraction as the gold standard. Clinical and translational gastroenterology 10 (2019): 00081

31. Hsu P, Wu L, Yen H, et al. Attenuation imaging with ultrasound as a novel evaluation method for liver steatosis. Journal of clinical medicine 10 (2021): 965.

32. Fujiwara Y, Kuroda H, Abe T, et al. The B-mode image-guided ultrasound attenuation parameter accurately detects hepatic steatosis in chronic liver disease. Ultrasound Med Biol 44 (2018): 2223-2232.

Chiyanika C, et al., Arch Clin Biomed Res 2023
DOI:10.26502/acbr.50170368

33. Yoo J, Lee JM, Joo I, et al. Reproducibility of ultrasound attenuation imaging for the noninvasive evaluation of hepatic steatosis. Ultrasonography 39 (2020): 121.

34. Jeon SK, Lee JM, Joo I, et al. Prospective evaluation of hepatic steatosis using ultrasound attenuation imaging in patients with chronic liver disease with magnetic resonance imaging proton density fat fraction as the reference standard. Ultrasound Med Biol 45 (2019): 1407-1416.

35. Ferraioli G, Monteiro LBS. Ultrasound-based techniques for the diagnosis of liver steatosis. World journal of gastroenterology 25 (2019): 6053.

36. Ferraioli G, Maiocchi L, Savietto G, et al. Performance of the attenuation imaging technology in the detection of liver steatosis. Journal of Ultrasound in Medicine 40 (2021): 1325-1332.

37. Welman CJ, Saunders J, Zelesco M, Abbott S, Boardman G, Ayonrinde OT. Hepatic steatosis: Ultrasound assessment using attenuation imaging (ATI) with liver biopsy correlation. Journal of Medical Imaging and Radiation Oncology 67 (2023): 45-53.

38. Hsu P, Wu L, Yen H, et al. Attenuation imaging with ultrasound as a novel evaluation method for liver steatosis. Journal of clinical medicine 10 (2021): 965.

39. Yoo J, Lee JM, Joo I, et al. Reproducibility of ultrasound attenuation imaging for the noninvasive evaluation of hepatic steatosis. Ultrasonography 39 (2020): 121.

40. Bae JS, Lee JM, Park S, Lee KB, Han JK. Magnetic resonance elastography of healthy livers at 3.0 T: Normal liver stiffness measured by SE-EPI and GRE. Eur J Radiol 107 (2018): 46-53.

41. Bae JS, Lee DH, Lee JY, et al. Assessment of hepatic steatosis by using attenuation imaging: A quantitative, easy-to-perform ultrasound technique. Eur Radiol 29 (2019): 6499-6507.

42. Ferraioli G, Soares Monteiro LB. Ultrasound-based techniques for the diagnosis of liver steatosis. World J Gastroenterol 25 (2019): 6053-6062.

43. Jeon SK, Lee JM, Joo I, et al. Prospective evaluation of hepatic steatosis using ultrasound attenuation imaging in patients with chronic liver disease with magnetic resonance imaging proton density fat fraction as the reference standard. Ultrasound Med Biol 45 (2019): 1407-1416.

44. Tamaki N, Koizumi Y, Hirooka M, et al. Novel quantitative assessment system of liver steatosis using a newly developed attenuation measurement method. Hepatology Research 48 (2018): 821-828.